©1998 The Visualization Society of Japan and Ohmsha, Ltd.
Journal of Visualization, Vol. 1, No. 2 (1998) 217-226

# An Analysis of Noise in PIV Images

Bugg, J. D.* and Rezkallah, K. S.*

* Department of Mechanical Engineering, University of Saskatchewan, Saskatoon, Saskatchewan, Canada.

Received 20 March 1998.
Revised 19 June 1998.

***Abstract*:** Particle Image Velocimetry can provide detailed velocity field information that has unparalleled value to both experimentalists and computational fluid dynamicists. As with any measurement technique, it is important to assess the error associated with the measurements.

The PIV measurement chain contains several stages where error is introduced. The dynamics of the seed particles determine how well they represent the local fluid velocity. Acquiring the image, whether photographically or electronically, will introduce aberrations, distortion, diffraction, and positioning uncertainties. The image analysis procedure to determine particle displacements is the final step in the measurement chain. This paper considers the error in this step of the measurement chain.

Synthetic images were generated with controlled levels of the following quantities: background mean illumination, background illumination standard deviation, mean particle diameter, number of paired particles, the ratio of unpaired particles to paired particles, displacement magnitude, and displacement direction. The analysis method tested is a generic autocorrelation technique using a two-dimensional forward FFT, PSD calculation, inverse FFT, and a peak detection algorithm based on a decreasing threshold search with subsequent sub-pixel interpolation. The error analysis principles demonstrated, however, could easily be applied to other algorithms including those implementing cross-correlation techniques.

The error in the analysis technique is characterised by four quantities: the bias in the displacement magnitude, the precision index of the displacement magnitude, the bias in the displacement direction, and the precision index of the displacement direction. Each independent variable was varied over a specified range and the behaviour of the four dependent variables observed.

The results showed a clear ability for this error assessment technique to illustrate the reliable operating range for each parameter. The variation in error with parameter level tended to be similar in all cases. There was a significant portion of the range where the error was very low. Then, at some critical value, the analysis technique broke down and the error became quite high.

***Keywords*:** particle image velocimetry, error analysis.

## *Nomenclature*:

| | |
|---|---|
| $B$ | Bias limit |
| $I_o$ | Intensity at centre of particle |
| $I$ | Intensity of particles |
| $N$ | Number of particles |
| $\vec{R}$ | Displacement |
| $R$ | Displacement magnitude |
| $r$ | Distance from centre of particle |
| $S$ | Precision index |
| $U$ | Uncertainty |
| $z$ | Autocorrelation function |

***Greek***

| | |
|---|---|
| $\Delta i$ | Pixel displacement of autocorrelation peak |
| $\Delta j$ | Pixel displacement of autocorrelation peak |
| $\eta$ | Local coordinate axis |
| $\mu$ | Mean |
| $\sigma^2$ | Variance |
| $\theta$ | Displacement direction |
| $\xi$ | Local coordinate axis |

***Subscripts***

| | |
|---|---|
| $b$ | Background |
| $D$ | Particle diameter |
| $I$ | Image intensity |
| $i$ | Pixel grid index |
| $j$ | Pixel grid index |
| max | Location of peak in autocorrelation function |
| $p$ | Paired particles |
| $s$ | Spurious particles |

# 1. Introduction

Particle Image Velocimetry (PIV) holds tremendous potential as a tool for validating computational fluid dynamics predictions and for understanding fluid flow from a purely experimental perspective. Proper error analysis of PIV images is essential to place the technique on a firm foundation and establish credibility. PIV can be subdivided into two tasks, image acquisition and image analysis. This paper is concerned with an error analysis of the second stage of this process. The images to be analysed, however, will possess many of the sources of error introduced during the image acquisition stage.

Comprehensive reviews of PIV are given by Adrian (1986) and Adrian (1991) and the details will not be repeated here. Some specific work on error analysis in PIV is available in the literature. Guezennec & Kiritsis (1990) presented work which analysed the error in a particle tracking algorithm. This algorithm used histogramming, local filtering, and thresholding on the original image in an attempt to produce binary intensity images. The critical stage of choosing a threshold was discussed at some length. After thresholding, cross-correlation techniques were applied to sub-regions of the image to estimate the local velocity. This local velocity was then used to give the expected position of the second image of a particle. A refined search was then done to find the particle shift with sub-pixel accuracy. The images so analysed were synthetic. Error was reported as a function of several parameters describing the image. Image contrast was identified as the most important. Image contrast was defined as the difference in illumination amplitude between the particles and the background. The error reported made no distinction between bias and precision index. Also, although a variety of flow directions were clearly examined, no comments are apparent about the effect of direction on accuracy.

Willer & Gharib (1991) analysed the error in a digital PIV system by mechanically translating an image in front of the recording camera. They reported the RMS fluctuation of the measurement versus both seeding density and particle displacement. This technique illustrated their analysis procedure to be very impressive, achieving an uncertainty of less than one tenth of a pixel over a displacement range of two orders of magnitude.

Keane & Adrian (1990) present a detailed study of the effect of seven dimensionless quantities on the valid detection probability of double pulsed PIV. Their work assumed uniform diameter particles and no background noise. A Monte Carlo simulation using ensembles of 1200 simulated images were used. They reported the effect of out-of-plane motion and velocity gradients on the performance of conventional analysis techniques. In addition to recommending optimal values of the various dimensionless parameters, they suggest an experimental design procedure that can be used to achieve good results.

# 2. Simulated Images

The images used in this paper to assess the error in the PIV image analysis procedure were synthetic. Each image represents a single interrogation area. All images were $64 \times 64$ pixels. Each pixel was represented by 8 bits corresponding to 256 levels of grey. The experimental technique simulated is assumed to use a double exposed

image of the measurement plane. The same error analysis technique could equally well be applied to dual frame data but that will not be addressed in this paper. All the particles on the simulated images had the same displacement, representing a region in a uniform velocity field.

Several parameters were used to quantify the characteristics of the simulated images.

1. *Background noise*: Before particles were placed on the simulated image the entire image was initialised with Gaussian noise with a specified mean intensity $\mu_b$ and variance $\sigma^2_b$.
2. *Number of paired particles*: These particles were placed randomly in the interrogation area and then copied a known distance in a known direction.
3. *Number of spurious particles*: Extra particles were placed randomly in the interrogation area to represent spurious particles in the image.
4. *Particle diameter*: The distribution of particle diameters was Gaussian with mean $\mu_D$ and variance $\sigma^2_D$. When a paired particle was copied to its second location the same diameter was used. The Gaussian distribution of particle sizes therefore represents the variation in actual particle sizes and not variations in the way that light may be reflected in the two exposures.
5. *Particle intensity*: The distribution of particle intensities was Gaussian with mean $\mu_{Io}$ and variance $\sigma^2_{Io}$ intensity at the centre of the particle images. The pixel intensity was calculated from the following with the particle radius being the distance from the centre to where the intensity falls to $1/e$ of its centreline value.

$$I = I_0 e^{-2r/\mu_D} \tag{1}$$

6. *Displacement magnitude*: In this work, every particle was given the same specified displacement.
7. *Displacement direction*: Every particle had the same specified displacement direction.

Several quantities in the image generation routine required a random number generator. A uniform random variable was required for positioning the first image of the paired particles and the unpaired particles. A Gaussian variate was required to set the background illumination, particle diameter, and particle illumination. Both of these generators are available in Press et al. (1988).

## 3. Analysis Routine

### *3.1 Autocorrelation Technique*

Since the image is assumed to come from a double exposed record, an autocorrelation technique was used to measure the particle displacement. This was done in the frequency domain by performing a forward FFT on the image, calculating the power spectral density, and then performing an inverse FFT to give the autocorrelation function.

### *3.2 Peak Finding*

The location of the proper peak in the autocorrelation function is critical to the technique and can occupy a very significant portion of the total analysis time. A progressively decreasing threshold technique was used here. The self-correlation peak corresponding to zero displacement is always the maximum in the autocorrelation function. Considering this magnitude to be unity, a threshold value was set which was initially a value slightly less than unity. The autocorrelation function was then searched to determine how many peaks penetrated through the threshold. Initially, only the self-correlation peak will be detected. The threshold value was then reduced slightly and the process was repeated. When the number of peaks penetrating the threshold increased to three, the search was halted. These three peaks correspond to the self-correlation peak and the two directionally ambiguous peaks representing the actual displacement. In this work no technique was implemented to resolve the directional ambiguity and both components of displacement were positive.

### *3.3 Sub-pixel Interpolation*

Sub-pixel accuracy is achieved in the present algorithm by a simple bi-quadratic interpolation on an array of pixel values including the identified relative maximum and its four nearest neighbours. Let $(\xi, \eta)$ be a local coordinate system with its origin at the relative maximum in the autocorrelation function identified by the procedure described in the previous section. A local bi-quadratic fit is

$$z = z_{i,j} + \frac{z_{i+1,j}+z_{i-1,j}}{2}\xi + \frac{z_{i,j+1}+z_{i,j-1}}{2}\eta + \frac{z_{i+1,j}+z_{i-1,j}}{2}\xi^2 + \frac{z_{i,j+1}+z_{i,j-1}}{2}\eta^2 \tag{2}$$

The maximum in the autocorrelation function $z$ can be found from

$$\left|\overrightarrow{\nabla z}\right| = 0 \tag{3}$$

which gives

$$\xi_{\max} = \frac{z_{i-1,j} - z_{i+1,j}}{2z_{i+1,j} - z_{i,j} + 2z_{i-1,j}} \tag{4}$$

$$\eta_{\max} = \frac{z_{i,j-1} - z_{i,j+1}}{2z_{i,j+1} - z_{i,j} + 2z_{i,j-1}} \tag{5}$$

The displacement $\vec{R}$ is

$$\vec{R} = (\Delta i + \xi_{\max})\hat{i} + (\Delta j + \eta_{\max})\hat{j} \tag{6}$$

where $\Delta i$ and $\Delta j$ are the displacements measured to the nearest pixel and ($\xi_{\max}$, $\eta_{\max}$) is the sub-pixel interpolation portion. This displacement can also be expressed in terms of a magnitude and direction.

$$\vec{R} = R(\cos\theta\hat{i} + \sin\theta\hat{j}) \tag{7}$$

## 4. Error Analysis

The purpose of the error analysis is to measure the uncertainty in both the magnitude and direction as a function of several parameters characterising image quality. In addition, these uncertainties are functions of the magnitude and direction of the displacement themselves. This uncertainty is composed of a bias and a random component so that

$$U = B + t_{95}S \tag{8}$$

where $B$ is the bias limit, $t_{95}$ is the value of the $t$ distribution at the 95% level of confidence, and $S$ is the precision index (standard deviation). As described by the ASME (1986) standard, this approach gives about 99% coverage of expected results. There are four quantities to be determined, the two bias limits $B_R$ and $B_\theta$, and the two precision indices $S_R$ and $S_\theta$. Specifically, information is sought about the functions

$$U_R = U_R(\mu_b, \sigma_b, \mu_D, N_P, N_S/N_P, R, \theta) \tag{9}$$

$$U_\theta = U_\theta(\mu_b, \sigma_b, \mu_D, N_P, N_S/N_P, R, \theta) \tag{10}$$

where $U_R$ and $U_\theta$ are the uncertainties in particle displacement magnitude and direction respectively. The quantities characterising the quality of the image given in Table 1 were selected as a preliminary list to investigate. The high and low levels of each parameter are given in Table 1 along with a level defining the base case. In all cases $\mu_{Io}$ = 200 and $\sigma_{Io}$ =20. Also the standard deviation of the particle diameter $\sigma_D$ was set at $\mu_D$/10, a value typical of PIV seed particles. Although the number of paired particles ($N_p$=35) chosen for the base case is somewhat higher than is typically used in PIV, the range chosen for this parameter spans that used in general practice.

All displacements are measured in pixels and all displacement directions are measured in degrees. For a given level of these parameters, an ensemble of simulated 64×64 images was generated. The members of the ensemble were made unique by seeding the random number generator with a different value. This made each image in the ensemble unique, but they still possessed the same statistical properties. Each image in the ensemble

Table 1 High, low, and base case levels of the seven parameters.

| Parameter | Low | Base | High |
|---|---|---|---|
| $\mu_b$ | 40 | 75 | 120 |
| $\sigma_b/\mu_b$ | 0.1 | 0.25 | 0.5 |
| $\mu_D$ | 1.0 | 3.0 | 5.0 |
| $N_p$ | 5 | 35 | 50 |
| $N_s/N_p$ | 0.0 | 1.5 | 5.0 |
| $R$ | 2.0 | 11.0 | 20.0 |
| $\theta$ | 0.0 | 22.5 | 45.0 |

was then analysed to measure the particle displacement and direction which was compared to the actual displacement and direction to yield a single measurement of the error. The mean of the measured error represents the bias while the standard deviation represents the precision index.

## 5. Results

A base case was defined as indicated in Table 1. An example baseline image generated with these parameters is shown in Fig. 1.

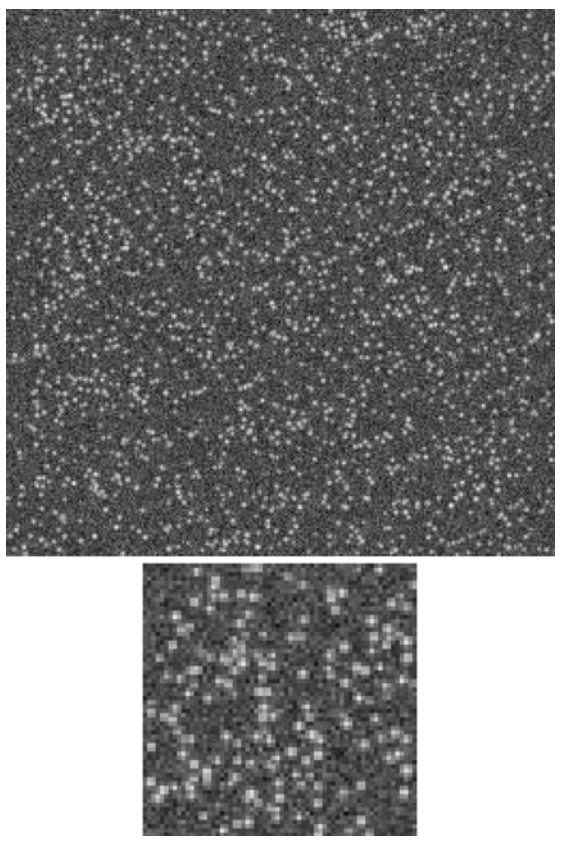

Fig. 1. Example images for base case. The top image is a composite of 16, 64×64 images. The bottom image is an expanded view of a single image.

The base case was used to investigate the number of images required in an ensemble of images to give reliable statistics. If the number of images in the ensemble is sufficient, repeating the process should yield the same values of $B$ and $S$. Five trials were done at each ensemble size. Each trial was made unique by using different seeds. Figure 2 shows the results of these runs. Only the displacement magnitude precision index $S_R$ is plotted. For small ensembles there is appreciable scatter in the results from one trial to another. However, as the number of members in the ensemble increased, the five trials gave essentially the same result. In order to ensure the results were independent of the ensemble size, all further runs in this paper were done with an ensemble size of 1024. The base case exhibited the biases, precision indices, and uncertainties indicated in Table 2.

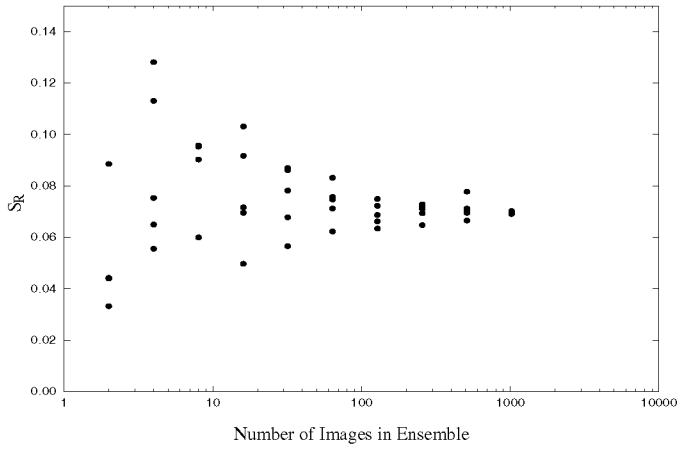


Fig. 2. The effect of sample size on the ability to calculate converged statistics.

Table 2 Summary of uncertainties for the base case.

| | Displacement | Orientation |
|---|---|---|
| $B$ | −0.12 | −0.36 |
| $S$ | 0.069 | 0.35 |
| $U^-$ | −0.25 | −1.0 |
| $U^+$ | 0.015 | 0.33 |

Each parameter was varied over the range indicated in Table 1 while the other parameters were held constant at the base value. The results of each of these tests are presented and discussed in this section. The ordinate on Fig. 3 through Fig. 9 has the general label “Error”. For the bias and precision index in displacement magnitude, this error is in pixels while for the bias and precision index in direction, this error is in degrees.

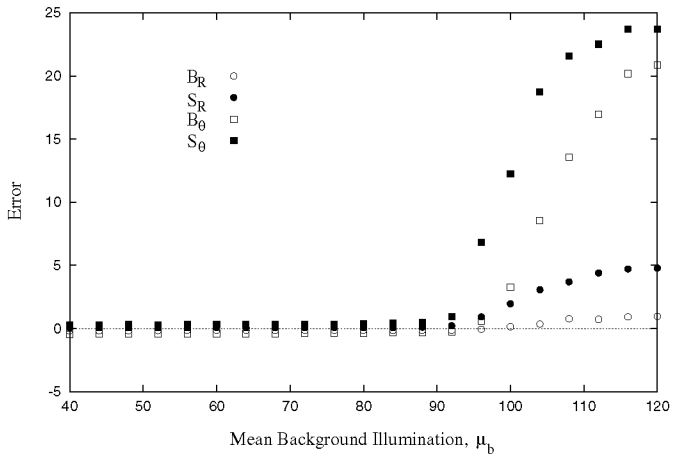


Fig. 3. The influence of background noise level on error.

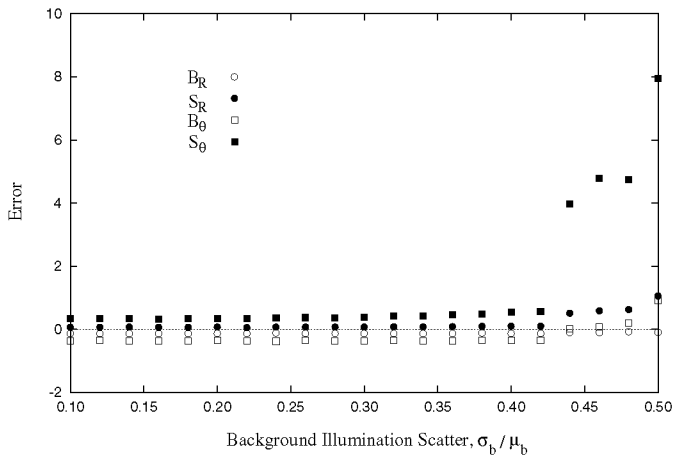


Fig. 4. The influence of background noise standard deviation on error.

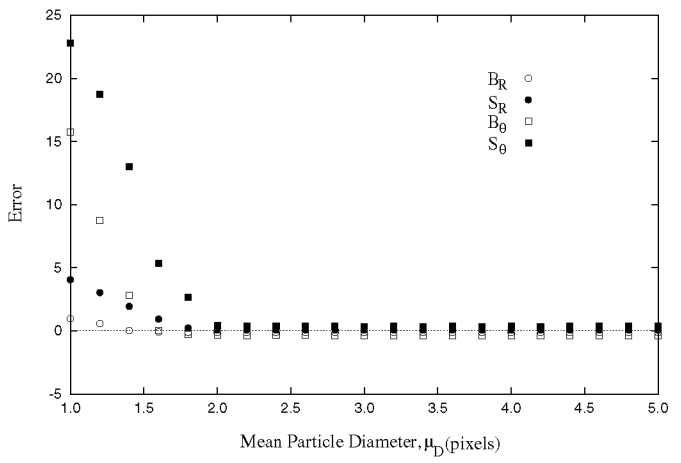


Fig. 5. The influence of particle diameter on error.

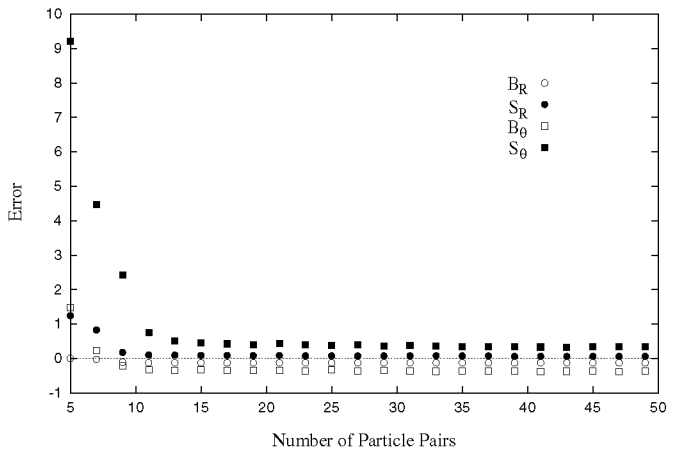


Fig. 6. The influence of number of particle pairs on error.

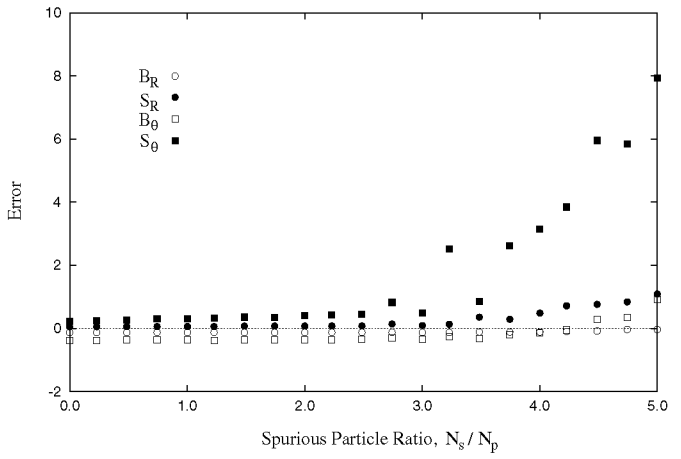


Fig. 7. The influence of spurious particle ratio on error.

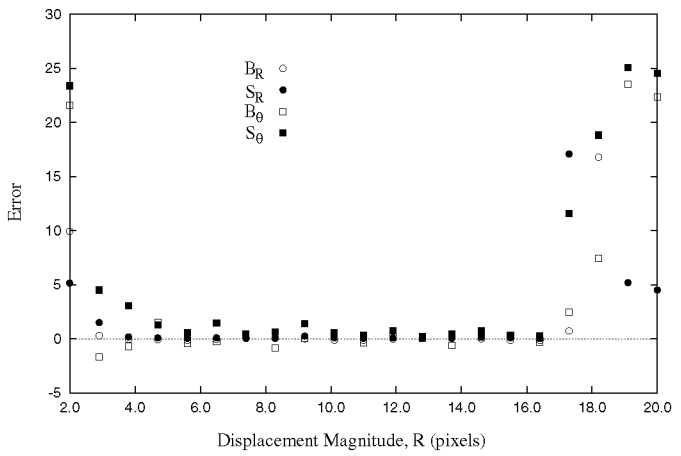


Fig. 8. The influence of particle displacement magnitude on error.

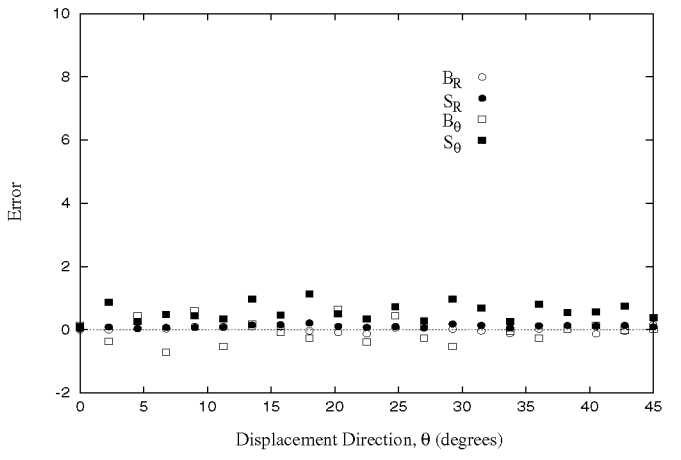


Fig. 9. The influence of particle displacement direction on error.

Figure 3 shows the variation in error with background noise level. This graph is representative of many of the graphs that will be presented in this section. There is a distinct region over which the error is very low, essentially any $\mu_b$ less than 90. Below this cutoff the error is very small. All runs in this paper were done with a mean particle illumination of 200. As $\mu_b$ is increased above 90 the technique fails quite dramatically. The high values of $B_\theta$ and $S_\theta$ at large $\mu_b$ indicate a complete failure of the analysis technique. Recall that both components of the velocity are positive in this work. The direction is essentially random within the $0^\circ$ to $90^\circ$ range possible. It is curious that the precision index of the displacement magnitude is so low in light of this. Figure 4 illustrates that increased variability in the background intensity has a similar effect to the background intensity itself. The same effect is likely responsible for both plots. The mean background level $\mu_b$ was held at 75 for Fig. 4. When the ratio $\sigma_b/\mu_b$ is 0.5 a significant portion of the background is going to be above the background illumination level of 90 which was identified in Fig. 3 as the upper limit on background intensity for a particle illumination of 200.

Figure 5 illustrates that mean particle diameters below two pixels cause the current technique to rapidly lose accuracy. However, above two pixels the sensitivity to particle diameter is minimal. The reason for this loss of accuracy relates to the illumination level of the particles. Although $I_o$ in Eq. (1) is 200, when the particle diameter is very small, the nearest pixel to the particle centre may have an illumination significantly less than 200. Effectively then, small particle diameters are behaving similar to large background illuminations because the ratio of particle intensity to background intensity reduces. The characteristics of Fig. 5 at low $\mu_D$ are very similar to Fig. 3 at high $\mu_b$.

Figure 6 and Figure 7 illustrate the influence of the number of particle pairs and the number of unpaired particles on the error. The current technique appears to be quite tolerant of heavy particle loads with no degradation in accuracy apparent up to 50 particle pairs in a $64\times64$ interrogation area. On the other hand, accuracy is lost if the number of particle pairs drops significantly below ten. The major effect appears to be a lot of scatter in the predicted direction. It is likely that with a small number of particles, ambiguity in the particle image pairing starts to become rather significant. The existence of spurious particles gives the expected result. High spurious particle counts clearly begin to degrade the measurement. This error analysis technique appears capable of identifying the number of spurious particles allowable. With knowledge of the out-of-plane velocity component, this would guide the selection of light sheet thickness and pulse separation.

The displacement magnitude has an important influence on the error. The results given here degrade at both a low displacement $R<3$ and a high displacement $R>17$. The particle diameter for these runs is at its base value of three pixels. This corresponds quite closely to the lower limit of allowable displacements since the particle images in successive exposures will begin to overlap. The upper limit on allowable displacement corresponds closely with the guideline that particle displacement be restricted to less than one quarter of the interrogation area (Keane and Adrian, 1990). Figure 9 illustrates that the error is essentially independent of the displacement direction.

All the results reported in this paper address only the influence of each parameter independently. Essentially, only the first order effects (eg. $\partial U_R/\partial\mu_b$) of the model functions (9) and (10) have been investigated and discussed. The coupled influences of these parameters are also important. However, the number of possible coupled influences for the seven parameters is substantial. An exhaustive study is beyond the scope of this paper. Figs. 3 through 9 all indicate a rather substantial region in the neighbourhood of the base case where the error is low. It is likely that coupled influences would also be weak in the region of the base case. However, if one simultaneously increased the background illumination $\mu_b$ while decreasing the particle size $\mu_D$, for example, we would certainly expect the accuracy to erode sooner than if the parameters were changed individually.

## 6. Conclusions

The technique of generating simulated PIV images to assess error in an analysis technique yields valuable information about the capabilities and expected performance limitations of the method. Care must be taken to consider a rather large number of simulated images ($\cong$1000) to obtain converged statistics. Also, it is valuable to consider both the bias and precision components of the uncertainty. In this work, the error analysis technique was applied to autocorrelation PIV. It was possible to identify the level of seven parameters were the method's accuracy broke down.

## Acknowledgments

The financial support of the Natural Sciences and Engineering Research Council of Canada is gratefully acknowledged. An early version of the routine to generate simulated images was written by G. Wright. N. Tischler's help with the peak finding algorithm is acknowledged.

## References

Adrian, R. J., Multi-point Optical Measurements of Simultaneous Vectors in Unsteady Flow - A Review, International Journal of Heat & Fluid Flow, 7(1986), 127-145.

Adrian, R. J., Particle-imaging Techniques for Experimental Fluid Mechanics, Ann. Rev. Fluid Mech., 23(1991), 261-304.

ANSI/ASME PTC 19.1-1985, Part 1, Measurement Uncertainty, The American Society of Mechanical Engineers (1986), New York.

Guezennec, Y. G. and Kiritsis, N., Statistical Investigation of Errors in Particle Image Velocimetry, Experiments in Fluids, 10(1990), 138-146.

Keane, R. D. and Adrian, R. J., Optimisation of Particle Image Velocimeters. Part I: Double pulsed systems, Measurement Science Technology, 1(1990), 1202-1215.

Montgomery, D. C., Design and Analysis of Experiments (Third Edition), (1991), John Wiley & Sons Inc.

Press, W. H., Flannery, B. P., Teukolsky, S. A., and Vetterling, W. T., Numerical Recipes in C: The Art of Scientific Computing, (1988), Cambridge University Press.

Willert, C. E. and Gharib, M., Digital Particle Image Velocimetry, Experiments in Fluids, 10(1991), 181-193.

## Authors' Profiles

Dr. Bugg is an Associate Professor of Mechanical Engineering at the University of Saskatchewan, Canada. He obtained his Ph.D. from the University of Calgary in 1991 in the area of bubble dynamics. His research interests are computational fluid dynamics and particle image velocimetry pertaining to fundamental studies of two-phase flow phenomena.

Dr. Rezkallah is a Professor of Mechanical Engineering at the University of Saskatchewan, Canada. In 1987, he obtained his Ph.D. from the University of Manitoba in the area of two-phase flow and heat transfer. In 1988, Dr. Rezkallah established the Microgravity Research Group. He has published extensively in this area, and has been the guest speaker in several national and international conferences and workshops.